Metric Driven RoSy Field Design and Remeshing

Yu-Kun Lai[a], Miao Jin[b], Xuexiang Xie[c], Ying He[c],
Jonathan Palacios[d], Eugene Zhang[d], Shi-Min Hu[a] and Xianfeng Gu[e]

Abstract—Designing rotational symmetry fields on surfaces is an important task for a wide range of graphics applications. This work introduces a rigorous and practical approach for automatic N-RoSy field design on arbitrary surfaces with user defined field topologies. The user has full control of the number, positions and indices of the singularities (as long as they are compatible with necessary global constraints), the turning numbers of the loops, and is able to edit the field interactively. We formulate N-RoSy field construction as designing a Riemannian metric, such that the holonomy along any loop is compatible with the local symmetry of N-RoSy fields. We prove the compatibility condition using discrete parallel transport. The complexity of N-RoSy field design is caused by curvatures. In our work, we propose to simplify the Riemannian metric to make it flat almost everywhere. This approach greatly simplifies the process and improves the flexibility, such that, it can design N-RoSy fields with single singularity, and mixed-RoSy fields. This approach can also be generalized to construct regular remeshing on surfaces. To demonstrate the effectiveness of our approach, we apply our design system to pen-and-ink sketching and geometry remeshing. Furthermore, based on our remeshing results with high global symmetry, we generate Celtic knots on surfaces directly.

Index Terms—metric, rotational symmetry, design, surface, parameterization, remeshing

1 Introduction

Many objects in computer graphics and digital geometry processing can be described by *rotational-symmetry fields*, such as brush strokes and hatches in non-photorealistic rendering, regular patterns in texture synthesis, and principal curvature directions in surface parameterizations and remeshing. N-way rotational symmetry (N-RoSy) fields have been proposed to model these objects. Formally, an N-RoSy field can be considered as a multi-valued vector field; at each position, there exist N vectors in the tangent space, each differed by a rotation of integer multiples of $\frac{2\pi}{N}$.

The most fundamental requirement for an N-RoSy field design system is to allow the user to fully control the topology of the field, including the number, positions and indices of the singularities, and the turning numbers of the loops [1], [2]. Automatic generation of N-RoSy fields with user prescribed topologies remains a major challenge.

The method in [1] generates fields with user defined singularities, but it also produces excess singularities, which requires further singularity pair cancellation and singularity movement operations. However, canceling singularities completely without significantly affecting the field is challenging. In general cases, cleaning up all the extra singularities is almost impractical. The method in [2] is the first one that guarantees the correct topology of the field, but for the purpose of generating smooth RoSy fields with specified singularities, it requires the user to provide an initial field with all singularities at the desired positions. In practice, finding such an initial field is the most challenging step. For example, a common user can hardly imagine a smooth vector field with only one singularity as shown in Figure 2 and Figure 8. Although such examples are extreme in some sense, fields with less singularities are often preferred, because singularities cause visual artifacts in real applications. Moreover, the power of our approach is that users can specify *any* number of singularities, with desired curvatures and positions, as long as the total Gaussian curvature of the surface is $2\pi\chi(S)$ (a topology-related constant), where $\chi(S)$ is the Euler characteristic of the surface. By using fewer singularities or placing singularities at invisible vertices (hidden by occlusion or hardly seen from practical viewpoints), artifacts can be significantly reduced.

In this work, we provide a rigorous and practical method which allows the user to design N-RoSy fields with full control of the topology (as long as they are compatible with global constraints such as the Gauss-Bonnet theorem and Poincaré-Hopf theorem) and without inputting any initial field. Furthermore, the algorithm can automatically generate a smooth field with the desired topology and allow the user to further modify it interactively.

1.1 Main Idea

Our method is based on the following intuition inspired by the work in [2]. An N-RoSy field has *local symmetry* that is invariant under rotations of an integer multiple of $\frac{2\pi}{N}$. A surface has *global symmetry*, which is intrinsically determined by

[a] *Tsinghua National Laboratory for Information Science and Technology, Department of Computer Science and Technology, Tsinghua University, Beijing, 100084, China*
[b] *Department of Computer Science, University of Louisiana at Lafayette, LA 70504, USA*
[c] *School of Computer Engineering, Nanyang Technological University, Singapore, 639798*
[d] *School of Electrical Engineering and Computer Science, Oregon State University, Corvallis, OR 97331, USA*
[e] *Department of Computer Science, Stony Brook University, Stony Brook, NY 11794, USA*

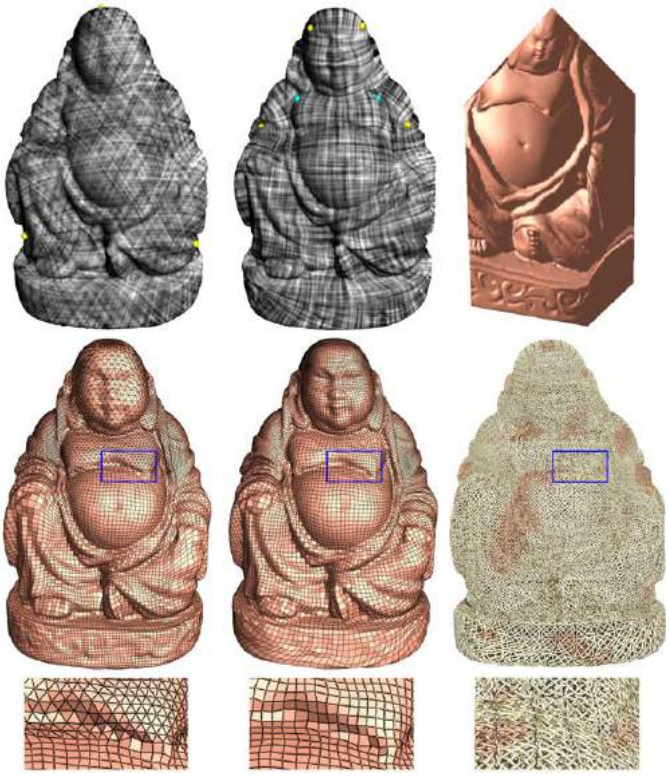

Fig. 1: *Metric-driven N-RoSy field design. From top left to bottom right, a 3-RoSy field, a 4-RoSy field, a flat cone metric visualized as an obelisk, triangle-quad mixed remeshing based on the metric, quad-remeshing, woven Celtic knot design over the surface based on the quad-remeshing. Close-ups are given for subfigures in the second row.*

the Riemannian metric. If the global symmetry is *compatible* with the symmetry of the N-RoSy fields, i.e. a metric is found such that the holonomy along any loop is a multiple of $\frac{2\pi}{N}$, then smooth N-RoSy fields can be constructed on the surface directly.

Roughly speaking, if a surface admits an N-RoSy field, then for any loop on the surface the total turning angle of the tangent vectors along the loop cancels the total turning angle of the N-RoSy field along the loop. Figure 7 provides such an example where a genus one polycubic surface admits 4-RoSy fields.

Most existing N-RoSy field design methods focus on adjusting the rotation of the field and keep the underlying surface untapped. While these approaches have been effective in some cases, it is difficult to enforce topological guarantees such as minimal number of singularities. Furthermore, these methods all require a constant N in the N-RoSy fields. In this paper, we describe a novel approach that modifies both the rotation of the field and the rotations of the loops by deforming the surface. Our work converts the problem of field design with user defined singularities to that of metric construction. The existence and uniqueness of the solution are guaranteed by the Circle Pattern theory in [3] and discrete Ricci flow in [4]. Existing works are based on 1-forms, energy minimization, and singularity movement/merging, and thus the theoretic argument for the existence of fields with exact singularity locations and indices is lack.

This approach greatly simplifies the process and produces results that are quite challenging for the alternatives, such as mixed-RoSy fields and remeshing in Figure 1, as well as fields with only one singular point in Figures 2 and 8. We further notice the distinction between N-RoSy fields and regular remeshing (without T-vertices): field design sets constraints to the rotational component of the holonomy, while remeshing sets constraints not only in rotational component, but also in translational component (i.e. generalized holonomy). Based on this, we are able to produce compatible metric that admits regular remeshing, as shown in Figure 1 and related Celtic knots in Figures 13 and 16.

1.2 Algorithm Pipeline

Our algorithm pipeline can be summarized as follows. In the first stage, an initial smooth vector field is constructed with the following steps: 1. the user specifies the desired singularities of the vector field; 2. we compute a flat cone metric, such that all the cone singularities coincide with those of the field; 3. we parallel transport a tangent vector at the base point to construct a parallel vector field; 4. if the parallel field has jumps when it goes around handles or circulates singularities, we apply two methods to eliminate the jumps: *rotation compensation* adjusts the rotation of the vector field; *metric compensation* modifies the rotation of the loops by deforming the surface. In the second stage, the vector field is further modified. we interactively edit the rotation and the magnitude of the vector field to incorporate user constraints.

Figure 2 illustrates the pipeline using rotation compensation method. (a)-(e) correspond to the first stage, while (f) and (g) correspond to the second stage. (a) User specifies the desired singularities with both positions and indices (Step 1). Here only one singularity is specified at the blue point with index -2. The curves are homotopy group basis. (b) We compute a flat metric, the curvature at the singularity is -4π, everywhere else 0 (Step 2). The surface is cut along the base curves and flattened to the plane. Note that the boundaries of the same color can match each other by a rigid motion. Practical algorithm for the purpose of field design does not need to explicitly flatten the whole surface onto a parameter domain. (c) We pull back the parallel vector field in the parameter domain onto the surface (Step 3). The field has discontinuities along the red curve, which corresponds to where "wave fronts" meet. It has no relation with the initial cut, only the result of holonomy. (d) We compute a harmonic 1-form to compensate the holonomy. (e) The smooth vector field is obtained after rotation compensation (Step 4). A smooth N-RoSy field has been constructed after the first stage. (f)(g) User inputs geometric constraints (red arrows) to guide the direction of the field, then the field is modified from (f) to (g).

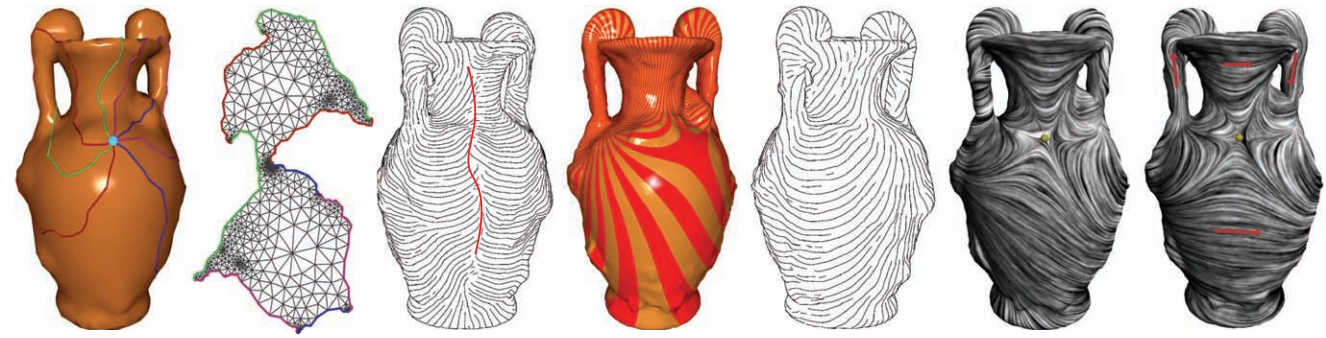

Fig. 2: *Algorithm pipeline.*

1.3 Contributions

In this work, *holonomy* plays the central role, which refers to the total turning angle of the tangent vectors along a loop. Holonomy represents the global symmetry of the surface. This work introduces a metric-driven method for N-RoSy field design (and remeshing). The major goal is to make the global symmetry of the metric represented as holonomy to be compatible with the local symmetry of N-RoSy field.

- We convert the N-RoSy field design problem (and remeshing problem) to flat cone metric design with constrained holonomy, and propose to use flat cone metric to simplify holonomy and improve the efficiency and efficacy of the algorithm. Furthermore, we give an explicit compatibility condition for a parallel N-RoSy field with the metric and generalize it for symmetric tessellations.
- We give rigorous and practical algorithms to construct N-RoSy fields with user fully controlled singularities on general surfaces. The method produces RoSy fields with arbitrary homotopy types, without excess singularities, and even with mixed-RoSy types. The algorithm is automatic and allows interactive editing.

Furthermore, we apply our remeshing method for the geometric texture construction application to weave Celtic knotwork on general surfaces, which requires highly global symmetry.

Note that this work focuses on the design and manipulation of metrics, which is different from other published methods for RoSy (or vector) field design. The reason to use new metric is to simplify the computation of holonomy. If the original metric is used, different loops have different holonomies. The dimension of the loop space is infinite, therefore the computation of all holonomy group is intractable. Using the new metric, the homotopic loops share the same holonomy, so the dimension of the homotopy group is finite. Metric design is a powerful tool and has the potential of being utilized for other graphics applications.

The organization of the paper is as follows. In Section 2, we briefly review the most related works. In Section 3 we give a brief introduction of the major concepts in Riemannian geometry and generalize them to discrete surfaces, and describe the theories for the compatibility between N-RoSy and metric. In Section 4, we explain the algorithm in detail. Finally we report our experimental results in Section 5 and conclude in Section 6 with insights and future directions of research. All the proofs of our theoretic results can be found in the appendix.

2 Previous Work

There has been a significant amount of work in the analysis and design of N-RoSy fields, especially when $N = 1$(vector) and 2(tensor). For a survey, we refer the readers to Palacios and Zhang [1] and references therein. Here, we will only mention the most relevant work.

There have been a number of vector field design systems for surfaces, most of which are generated for a particular graphics application such as texture synthesis [5]–[7], fluid simulation [8], and vector field visualization [9], [10]. Systems providing topological control include [11], [12]. The system of Zhang et al. has also been extended to create periodic orbits [13] and to design tensor fields [14]. Fisher et al. introduce a vector field design algorithm based on discrete exterior calculus [15], which produces smooth fields incorporating user constraints interactively through weighted least squares.

There has been some work on N-RoSy fields when $N > 2$. Hertzmann and Zorin [16] and Ray et al. [17] demonstrate that 4-RoSy fields are of great importance in surface illustration and remeshing, respectively. Both works also develop algorithms that can smooth the 4-RoSy fields in order to reduce the noise in the fields. Later, Ray et al. [2] provide the analysis of singularities on N-RoSy's by extending the Poincaré-Hopf theorem as well as describe an algorithm in which a field with a minimal number of singularities can be constructed based on user-specified constraints and the Euler characteristic of the underlying surface [2]. This is the first algorithm for direction field design that guarantees the correctness of the topology of the field. Palacios and Zhang provide comprehensive analysis for rotational symmetry fields on surfaces and present efficient algorithms for locating singularities, separatrices, and effective design operations in [1].

For previous methods [1], [2], [15], [18], [19], designing an N-RoSy field with a single singularity as shown in Figure 2 and Figure 8 will be very challenging. The method in [1] involves complex singularity movement and merging, and can not guarantee the topology of the field. The method in [18] is based on harmonic forms, which is efficient, but can not fully control the locations of singularities, and it is not clear how to construct general N-RoSy fields, such as $N = 3$. Kälberer et al. [19] require the construction of complex branched covering, which converts N-RoSy field design to vector field design on the covering space. Constructing a smooth vector field with global continuity on the covering space is based on harmonic forms, thus it also suffers from the lack of full control of the singularities. The technique of [15] is based on holomorphic 1-forms. The zero points of the 1-forms are intrinsically determined by the conformal structure and can not be fully controlled by the users, either. Ray et al.'s method [2] is not guaranteed to find the global minimum with respect to the discrete variables. Our work is fundamentally different in that, our method generates fields with exact locations and indices of singularities as specified, no extra singularity will appear; this can be rigorously proved. Compared with [2], by using flat cone metric, holonomy is defined on the finite-dimensional fundamental group, while in their work, holonomy is defined on the infinite-dimensional loop space. Thus, the theoretic argument and holonomy computation in our setting are greatly simplified. We further consider a related, but much more difficult problem of regular remeshing without T-vertices.

2.1 Pen-and-ink Sketching of Surfaces

Pen-and-ink sketching of surfaces is a non-photorealistic style of shape visualization. The efficiency of the visualization and the artistic appearance depend on a number of factors, one of which is the direction of hatches. Girshick et al. [20] show that 3D shapes are best illustrated if hatches follow principal curvature directions. However, curvature estimation on discrete surfaces is a challenging problem. While there have been several algorithms that are theoretically sound and produce high-quality results [16], [21]–[23], most of them still rely on smoothing to reduce the noise in the curvature estimate. Consequently, these methods do not provide control over the singularities in the field. Hertzmann and Zorin [16] propose the concept of cross fields, which are 4-RoSy fields obtained from the curvature tensor (a 2-RoSy field) by removing the distinction between the major and minor principal directions. They demonstrate that smoothing on the cross field tends to produce more natural hatch directions than smoothing directly on the curvature tensor. Their original goal is to smooth the field, and their method can not be directly used to control the singularities, although they also point out the fundamental need to control the number and location of the singularities in the field. Zhang et al. [14] address this issue by providing singularity pair cancelation and movement operations on the curvature tensor field. However, their technique cannot handle a 4-RoSy field.

2.2 Texture synthesis

In [7], 2 and 4-symmetry direction fields are used to steer synthesizing using 2 and 4-symmetry texture samples. [24] steer their texture generation method using a direction field defined as the gradient of a fair Morse function (it has the same singular points as the function). Based on the study of the Morse complex of smooth harmonic functions [25], this allows a user-controllable number and configuration of singularities. The gradient of the harmonic function is a direction field. The first work on computer generated Celtic knot was introduced by Kaplan and Cohen in [26]. [27] introduces mesh quilting method for geometric texture synthesis through local stitching and deformation. Our method for constructing Celtic knots on surfaces is a global method without partitioning the surface and stitching the texture patches.

2.3 Quad-Dominant Remeshing

The problem of quad-dominant remeshing, i.e., constructing a quad-dominant mesh from an input mesh, has been a well-studied problem in computer graphics. The key observation is that a nice quad-mesh can be generated if the orientations of the mesh elements follow the principal curvature directions [28]. This observation has led to a number of efficient remeshing algorithms that are based on streamline tracing [28]–[30]. Ray et al. [17] note that better meshes can be generated if the elements are guided by a 4-RoSy field. They also develop an energy functional that can be used to generate a periodic global parameterization and to perform quad-based remeshing. The connection between quad-dominant remeshing and 4-Rosy fields has also inspired Tong et al. [18] to generate quad meshes by letting the user design a *singularity graph* that resembles the behavior of the topological skeleton of a 4-RoSy field. On the other hand, Dong et al. [31] perform quad-remeshing using spectral analysis, which produces quad meshes that in general do not align with the curvature directions. A seminal method is introduced in [19], which converts a 4-RoSy field on a surface to a vector field by using 4 layer branched covering.

2.4 Metric Design

Kharevych et al. used circle patterns for discrete conformal mappings in [3]. The Euclidean flat cone metric with user prescribed singularities can be obtained by two stages: computation of per-edge angle to incorporate the input geometry, and solving circle radii with energy minimization. The edge angles together with computed radii determine the metric, using circle patterns. Jin et al. used circle packing to design flat cone metrics in [4], which handles spherical, Euclidean and hyperbolic discrete metrics. The algorithm is the discrete analogy of Ricci flow [32]. A linear metric scaling method for computing Euclidean flat cone metric with prescribed curvatures is introduced in [33], where the cone singularities can be automatically selected to minimize the distortion. Based on the work by Luo [34], Springborn et al. [35] improved the

accuracy of [33] and produced precise results by minimizing a convex energy function, which is a non-linear method. Circle pattern and discrete Ricci flow are also non-linear methods, require a preprocessing stage, and get an accurate metric; the metric scaling method is linear and flexible for general meshes but with less accuracy.

3 Theoretic Foundations

In this section, we first briefly introduce Riemannian geometry theories, and then generalize them to discrete settings. Next we present our major theoretical results. The detailed proofs can be found in the Appendix.

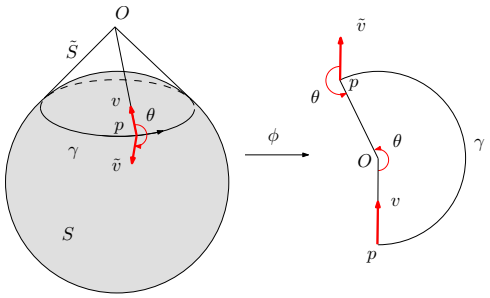

Fig. 3: *Parallel transport and holonomy. θ is the holonomy along γ.*

3.1 Basic Concepts in Riemannian Geometry

In order to quantitatively measure the rotation of a vector field along a curve and the rotation of curve itself on a surface, we need to introduce some tools from Riemannian geometry.

Parallel transport on a curved surface plays the central role. Suppose γ is a curve on the surface S. The envelope of all the tangent planes along γ is a developable surface $\tilde{S}$. We develop the envelope to the plane, so that γ becomes a planar curve. Suppose $\mathbf{v}$ is a tangent vector at a point p, we translate it to $\tilde{\mathbf{v}}$ on the plane along the development of γ. This corresponds to the parallel transport on the surface. The angle between the resulting transported vector and the initial vector is called the rotational component of the **holonomy** along γ, or simply the holonomy of γ. Holonomy describes the global symmetry of the surface. Figure 3 illustrates a parallel transport on a sphere S, where γ is a circle, $\tilde{S}$ is a conic surface, angle θ is the holonomy along γ.

Suppose a vector field $\mathbf{v}$ (in red) is along a path γ, connecting p and q. We parallel transport the tangent vector at the starting point p to the ending vertex q, this parallel vector field is $\mathbf{w}$ in blue. The rotation θ from $\mathbf{w}(q)$ to $\mathbf{v}(q)$ is called the *absolute rotation* of the vector field $\mathbf{v}$ along the path γ. The absolute rotation of the tangent direction of γ is equal to its holonomy. The *relative rotation* of the vector field $\mathbf{v}$ along the path γ is the difference between the absolute rotation of $\mathbf{v}$ and the holonomy of γ, which indicates the change of the angle between $\mathbf{v}$ and the tangent vector of γ along γ. The **compatibility condition** for a smooth N-RoSy field on a surface is that for any loop γ, the relative rotation of $\mathbf{v}$ along γ is an integer times of $\frac{2\pi}{N}$. Our central task is to make the absolute rotation of a vector field and the holonomy to cancel out each other.

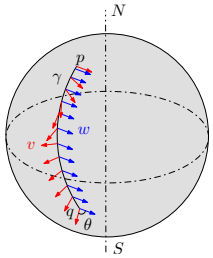

Fig. 4: Absolute rotation.

Parallel transport and holonomy along loops on curved surfaces are very complicated, which contributes to the difficulty of N-RoSy design. For example, if γ is the boundary of a surface patch Ω, then the holonomy of γ equals to the total curvature on Ω, $\int_\Omega K$, where K is the Gaussian curvature. Therefore, the parallel transport is path dependent. If K is zero everywhere, namely, the surface is flat, then parallel transport is path independent. The surface global symmetry is extremely easy to analyze. Unfortunately, according to the Gauss-Bonnet theorem, the total Gaussian curvature of the surface is a constant $2\pi\chi(S)$, where $\chi(S)$ is the Euler characteristic of the surface. If the surface is not of genus one, then its Riemannian metric cannot be flat everywhere.

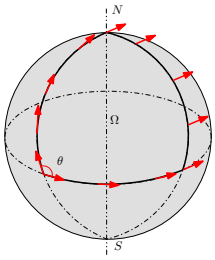

Fig. 5: Holonomy vs. curvature.

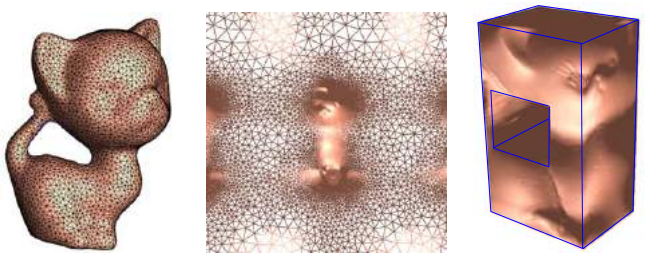

Fig. 6: *Flat cone metrics on a genus one kitten mesh. The first metric has no cone singularities, the second metric has* 16 *cone singularities, i.e.corners of polycube.*

Fortunately, we can design a **flat cone metric** of an arbitrary surface, such that the curvature is zero almost everywhere except at finite number of cone singularities. Let $\mathbf{g}$ be the induced Euclidean metric tensor on S. Suppose a user has selected the position and curvatures of the singularities on a surface, the target curvature is $\bar{K}$, then the target metric can be deformed by the Hamilton's surface Ricci flow [32], $\frac{d\mathbf{g}(t)}{dt} = (\bar{K} - K_{\mathbf{g}(t)})\mathbf{g}(t)$. Figure 6 demonstrates two different flat cone metrics of a genus one surface obtained by using Ricci flow.

3.2 Discrete Theories

All the aforementioned Riemannian geometric concepts are defined on smooth surfaces. In the following, we generalize the major concepts to the discrete settings.

Let M be a triangular mesh in $\mathbb{R}^3$. A *metric* of M is a configuration of edge lengths, such that the triangle inequality

holds on all faces. The *vertex curvature* is the angle deficit, i.e., 2π-the total angle around the vertex. A *flat cone metric* is a metric such that the curvatures are zero for almost all the vertices, except at a few ones. The vertices with non-zero curvatures are called the *cone singularities*. Note that metric determines curvatures. Reversely, in the discrete case, given the curvatures on vertices, we can uniquely determine a conformal metric (up to a scaling factor) using the methods in [3], [4], [33], [35]. The main concern to use such methods is because they can design metrics from prescribed curvatures, and thus we can accurately control the positions and indices of singularities of the field. Figure 6 shows two flat cone metrics for a genus one kitten model. The mesh is developed onto the plane by a flat metric without singularities. While the curvature is determined by the metric, the total curvature of the surface is determined by the topology of the mesh, which is equal to $2\pi\chi(M)$, where $\chi(M)$ is the Euler characteristic.

Let M be a mesh with a flat cone metric, and $S = \{s_1, s_2, \cdots, s_n\}$ be the cone singularity set. Let $\bar{M}$ denote the mesh obtained by removing all the cone singularities from M, $\bar{M} = M \backslash S$.

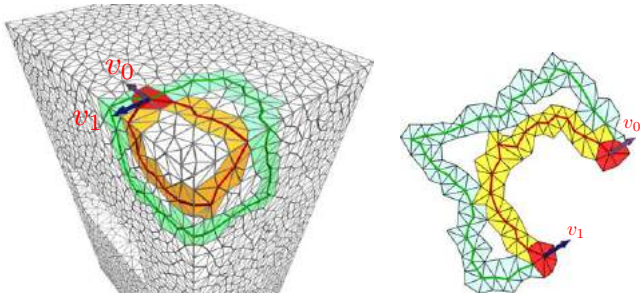

Fig. 7: *Discrete parallel transport and holonomy. Homotopic loops sharing the base vertex have the same holonomy.*

3.2.0.1 Parallel Transport: Parallel transport is the direct generalization of planar translation. Discrete parallel transport was introduced in [36] in the setting of geodesics on discrete surfaces. Let γ be a path consisting of a sequence of consecutive edges on $\bar{M}$, the sorted vertices of γ are $\{v_0, v_1, \cdots, v_n\}$. Let N_i denote the one-ring neighborhood of v_i (the union of all the faces adjacent to v_i), then the one-ring neighborhood of γ is defined as the union of all N_i's: $N(\gamma) = \bigcup_{i=0}^{n} N_i$.

The *development* of $N(\gamma)$ refers to the following process: first we flatten N_0 on the plane, and then we extend the flattening to N_1, such that the common faces in both N_0 and N_1 coincide on the plane. This process is repeated until N_n is flattened. In this way, we develop $N(\gamma)$ to the plane. We denote the development map as $\phi : N(\gamma) \to \mathbb{R}^2$. Note that the restriction of the development map on each triangle is a planar rigid motion. *Parallel transport* on the mesh along γ is defined as the translation on the development of $N(\gamma)$. See Figure 7 for the illustration of parallel transport.

3.2.0.2 Holonomy: In practice, we are more interested in the *loop* case, i.e. $v_0 = v_n$. When parallel transporting a tangent vector at v_0 along γ to v_n, the resulting vector differs from the original vector by a rotation, which is the *holonomy* of the loop, denoted as $h(\gamma)$. Given a vector field $\mathbf{v}$ along γ, we parallel transport the vector at the starting point. The vector at the ending point differs from the transported vector, which is the *absolute rotation* of the field along γ, denoted as $R_{\mathbf{v}}(\gamma)$.

Two loops γ_1, γ_2 sharing a base point p are *homotopic*, if one can deform to the other. The concatenation of γ_1, γ_2 through p is still a loop, which is the product of them. All homotopy classes of loops form a group, the so-called homotopy group $\pi(\bar{M})$. Suppose M has g handles, and n cone singularities. Then the basis of $\pi(\bar{M})$ is depicted in Figure 9, where each handle has two loops a_k, b_k, and each singularity s_i normally has one loop c_i. Note that in Figure 9, the loop around the center singularity is not included as a basis in the homotopy group, as this loop can be easily generated by the combination of all other marked loops. Details are explained in [2].

Homotopic loops have the same holonomy if the underlying surface has a flat cone metric. In this case, we can define the *holonomy map*, $h : \pi(\bar{M}) \to SO(2)$, where $SO(2)$ is the rotation group in the plane. Its image $h(\pi(\bar{M}))$ is the *holonomy group* of M, denoted as $holo(\bar{M})$.

3.2.0.3 Compatibility: **N-RoSy** The *relative rotation* of a vector $\mathbf{v}$ along γ is defined as the difference of the absolute rotation of $\mathbf{v}$ and the holonomy of γ, $T_{\mathbf{v}}(\gamma) = R_{\mathbf{v}}(\gamma) - h(\gamma)$. The relative rotation is equivalent to the *turning number* defined by [2]. Ray et al. proved that for a smooth N-RoSy field, the turning number along any loop must be integer times of $\frac{2\pi}{N}$.

$$T_{\mathbf{v}}(\gamma) = R_{\mathbf{v}}(\gamma) - h(\gamma) \equiv 0, mod \frac{2\pi}{N}. \tag{1}$$

Furthermore, the turning numbers on a basis of the homotopy group $\pi(\bar{M})$

$$\{T_{\mathbf{v}}(a_1), T_{\mathbf{v}}(b_1), \cdots, T_{\mathbf{v}}(a_g), T_{\mathbf{v}}(b_g), T_{\mathbf{v}}(c_1), \cdots, T_{\mathbf{v}}(c_n)\} \tag{2}$$

determine the homotopy class of the N-RoSy field. We develop our theoretical results based on these fundamental facts. All the proofs are given in the appendix.

The following theorems lay down the theoretical foundation of our metric-driven method, which claims that the topological properties of a vector field are preserved by metric deformation.

Theorem 3.1: Suppose $\mathbf{v}$ is a smooth N-RoSy field on a surface M. $\mathbf{g}(t)$ is a one parameter family of Riemannian metric tensors. Then for any closed loop γ on M, the relative rotation $T_{\mathbf{v}}(\gamma)$ on $(M, \mathbf{g}(t))$, i.e. M with the metric $g(t)$, is constant for any t.

Thus, smooth metric deformation doesn't change the topology of the field. We can therefore choose a special metric to simplify the computation as much as possible, i.e. a flat cone metric.

The simplest N-RoSy field is the parallel field, the following theory leads us to design our algorithm.

Theorem 3.2: Suppose M is a surface with a flat cone metric. A parallel N-RoSy field exists on the surface, if and only if all the holonomic rotation angles of the metric are integer times of $\frac{2\pi}{N}$.

For genus zero closed surfaces, the curvature of cone singularities determine the holonomy.

Corollary 3.3: Suppose M is a genus zero closed surface with finite cone singularities. M has a parallel N-RoSy field, if and only if the curvature for each cone singularity is $\frac{2k\pi}{N}$.

According to this corollary, it is easy to verify the symmetry of platonic solids. If a platonic solid has N vertices, then the vertex curvature is $\frac{4\pi}{N}$, therefore the rotational homology group is generated by the rotation of angle $\frac{4\pi}{N}$, a $\frac{N}{2}$-RoSy field exists on it. For example, an octahedron is with 6 vertices and 3-RoSy; a dodecahedron is with 20 vertices and 10-RoSy.

The following existence theorem gurantees the existence of N-RoSy fields on surfaces with arbitrary flat cone metrics.

Theorem 3.4: Suppose M is a surface with flat cone metric, then there exists a smooth N-RoSy field.

Suppose $\tilde{M}$ is a branched covering of M (defined in [19]), then the holonomy group of $\tilde{M}$ is a subgroup of that of M, $\tilde{M}$ may have more N-RoSy fields with lower N. For example, in [19], M has a parallel 4-RoSy field, its 4-layer branch covering $\tilde{M}$ allows a parallel 1-RoSy field, namely, a vector field.

Tessellation We wish to generalize planar tessellation to general surfaces. If the symmetry of the metric on the surface is compatible with the symmetry of the planar tessellation, then the surface can be re-meshed according to the planar tessellation.

We generalize holonomy to include both translation and rotation. Figure 7 shows the concept. Given a loop γ, the starting vertex v_1 coincides with the ending vertex v_n, we develop its neighborhood $N(r)$ onto the plane, then the development of N_1 and that of N_n differs by a planar rigid motion, which is defined as the *general holonomy* along γ. Two loops sharing the common base vertex share the same general holonomy. Therefore, general holonomy maps the homotopy group to a subgroup of planar rigid motion $E(2)$. We denote the image as $Holo(\bar{M})$, and call it the *general holonomy group* of $\bar{M}$.

Suppose T is a tessellation of the plane $\mathbb{R}^2$, τ is a rigid motion preserving T, $\tau(T) = T$. The *symmetry group* of T is defined as

$$G_T = \{\tau \in E(2) | \tau(T) = T\}.$$

Theorem 3.5: Suppose M is with a flat cone metric, the holonomy group of $\bar{M}$ is $Holo(\bar{M})$, if $Holo(\bar{M})$ is a subgroup of G_T, then T can be defined on M.

4 ALGORITHM

SUPPOSE the user specifies topological and geometric constraints for the N-RoSy field: *topological constraint* means the singularities, including the number, positions and indices; *geometric constraint* means the directions and lengths of the fields at some regions on the surface.

For discrete computation on meshes, we assume that the N-RoSy field is piecewise linear; each vertex is assigned a representative vector from N possible directions. This is consistent with singularities, since they are naturally specified at certain vertices. As detailed later in the section, we construct vector fields on flat metric, where the tangent vectors are defined intrinsically, and there is no difference to define the tangent on vertices or on faces. When we pull back the planar field to the original mesh, we define the tangent plane at each vertex as the average of the surrounding face planes, as done before in [28] for smoothing tensor fields.

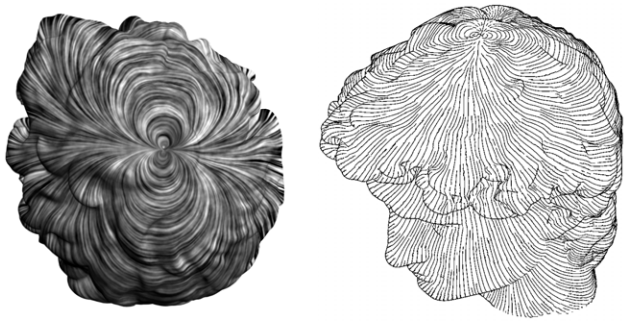

Fig. 8: *A vector field on a genus zero closed surface with a single singularity with index* $+2$.

Our algorithm has two major stages: stage one is to compute an initial N-RoSy field, which satisfies the topological constraints; stage two is to edit the N-RoSy field, locally rotate and scale the initial field to satisfy the geometric constraints.

4.1 Initializing N-RoSy Field

This stage has 3 steps: computing the metric, computing the holonomy, and holonomy compensation. For genus zero meshes, we only need the first step, because the metric will be compatible with N-RoSy fields automatically according to corollary 3.3.

4.1.1 Computing the Flat Cone Metric

The cone singularities are fully determined by the singularities on the desired N-RoSy field. Let v be a cone singularity, then its curvature and its index are closely related by the formula $Ind(v) = \frac{k(v)}{2\pi}$, where $Ind(v)$ is the index of v. Note that the Gaussian curvature at vertex v satisfies $K_v = 2\pi - \sum \tau_i$, where τ_i are top angles of 1-ring neighbors of v. Thus, if the index is less than 1 (i.e. the curvature is less than 2π), then it is easy to define the curvature of v. For vertex with an index greater than or equal to 1, it is more complicated to find the curvature, since the summation of the corner angles surrounding the vertex should be less than or equal to zero. We handle this situation in the following way. We punch a small hole at the cone singularity. Suppose the boundary vertices of the small hole are $\{v_1, v_2, \cdots, v_m\}$. Then the index of the

singularity and the total curvature of the boundary are related by $Ind(v) = \frac{\sum_{i=1}^{m} k_i}{2\pi} + 1$. Note that this is a problem all the algorithms will face; here we give a simple solution to the problem. Given the desired curvature, we can compute a flat metric using one of the conventional methods (e.g. the discrete Ricci flow method in [4]). Figure 8 illustrates a vector field constructed using this method on the Michelangelo's David head surface,which is a genus zero closed surface, with one singularity of index $+2$.

According to corollary 3.3, the flat cone metrics on a genus zero closed mesh satisfy the compatible condition automatically. Figure 10 shows one example, both 3-RoSy and 4-RoSy fields on a genus zero surface are constructed by parallel transport on the flat cone metric directly.

4.1.2 Computing the holonomy

For genus zero closed meshes, if the cone singularity curvatures satisfy the compatibility condition 1, then the flat cone metric of the surface satisfies the same condition. For high genus meshes, the cone singularity curvatures cannot guarantee the holonomy compatibility. This can be found by the example shown in Figure 2(c), where the metric on a genus two surface has a single cone singularity with curvature -4π, but the vector field constructed by parallel transport is not smooth. Thus, explicit computation (and compensation) of holonomy is required, as shown by the following example on a genus three surface.

We compute a basis of the homotopy group $\pi_1(\bar{M})$ using the method in [19]. The base loops are shown in Figure 9. Then we compute the development of each base loop γ to obtain the holonomy $h(\gamma)$. Please refer to Fig. 7 for an example of the development process. The holonomies of all the base loops form the generators of the holonomy group. For example, Figure 9 shows a genus three mesh with four cone singularities, which are labeled with different colors. The curvatures of the red, orange and blue singularities are $-\pi$,-3π,-2π, respectively. The holonomic rotation angles for c_1,c_2,c_3 are 0,π and 0 (modulo 2π).

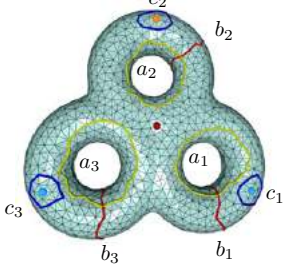

Fig. 9: Homotopy basis for a 3-hole torus with 4 singularities.

The holonomic rotation angles (with respect to a modulus of 2π) are as follows:

a_1	b_1	a_2	b_2	a_3	b_3
1.5551π	0.9683π	1.3704π	1.5175π	1.5975π	1.0574π

4.1.3 Holonomy Compensation

There are two methods for holonomy compensation, rotation compensation and metric compensation. The first one is to adjust the absolute rotation of the direction field $R_{\mathbf{v}}(\gamma)$; the second one modifies the metric to change the holonomy $h(\gamma)$,

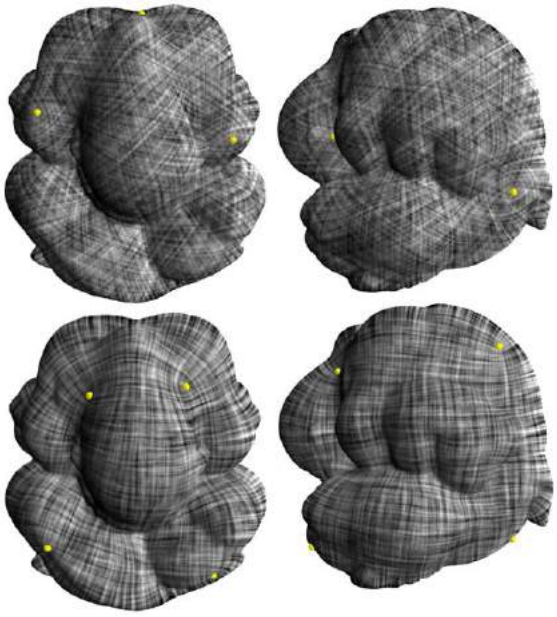

Fig. 10: *The Pensatore surface is a genus zero closed mesh. A 3-RoSy field is shown in the first row, where there are* 6 *cone singularities with the curvatures of* $\frac{2\pi}{3}$*. A 4-RoSy field is shown in the second row, there are* 8 *cone singularities with the curvatures of* $\frac{\pi}{2}$*.*

such that the relative rotation is equal to $\frac{2k\pi}{N}$ along arbitrary loops.

4.1.3.1 Rotation Compensation: This method is similar to the method in Ray et al. [2]. The rotation angle of the field is represented as a closed 1-form. The key difference is that, their method further rotates an existing *smooth* field and change the topology of the field; our method rotates a *non-smooth* field and make it smooth, it can also be applied to change the topology of a non-smooth field.

The homotopy class of the N-RoSy field is determined by the relative rotations on the basis of homotopy group in equation 2. We first use a conventional method [18] to compute a set of harmonic 1-form bases ω_k corresponding to the homotopy group generator γ_k. The mesh M is cut open along γ_k to obtain a new mesh M_k with two sides of γ_k denoted as γ_k^+ and γ_k^-, respectively. The harmonic function $g_k : M_k \to \mathbb{R}$ can be computed using

$$\Delta g_k = 0,$$

with the boundary conditions $g_k|_{\gamma_k^+} = 1$ and $g_k|_{\gamma_k^-} = 0$. We transfer the 1-form dg_k to M based on the edge correspondence, and find a function $h_k : M \to \mathbb{R}$, such that

$$\Delta(dg_k + dh_k) = 0.$$

Then, $\omega_k = dg_k + dh_k$ is one of the basis. Please refer to [18] for the detailed discussions. $\omega = \sum w_k \omega_k$ is a linear combination of all the bases, where w_k's are the weights to determine. To compute a harmonic 1-form ω on $\bar{M}$, such that for any homotopy group generator γ_k, the following condition

holds: for N-RoSy field design,

$$T_{\mathbf{v}}([\gamma_k]) - h([\gamma_k]) = \int_{\gamma_k} \omega = \int_{\gamma_k} \sum_k w_k \omega_k.$$

Solving a small linear system with w_k's as unknowns obtains the desired 1-form. Such a harmonic 1-form exists and is unique. Conceptually, the tangent field corresponding to the 1-form ω is constructed in the following way. We select a tangent vector w_0 at the base vertex. Suppose v is another vertex, the shortest path on $\bar{M}$ from v_0 to v is γ, then we parallel transport w_0 to v along γ to obtain w, then we rotate w clock-wisely about the normal by an angle $\theta = \int_\gamma \omega$. By this way, we propagate the tangent vector w_0 to cover the whole mesh.

In practice, we use an equivalent fast marching method to propagate the vector field.

1) Select a tangent vector w_0 at v_0, put v_0 in a queue.
2) If the queue is empty, stop. Otherwise, pop the head vertex v_i of the queue. Go through all the neighbors of v_i. For each neighboring vertex v_j, which hasn't been accessed, parallel transport w_i from v_i to v_j, rotate it counter-clock-wisely by angle $\omega(v_i, v_j)$. Enqueue v_j.
3) Repeat step 2, until all the vertices have been processed.

Figure 2 illustrates a vector field on a genus two amphora model with one singularity, computed using rotation compensation.

4.1.3.2 Metric Compensation: For designing smooth N-RoSy fields, automatic rotation compensation is already enough. For the purpose of remeshing, metric compensation method will be required. In contrast to rotation compensation, this approach modifies the flat cone metric to achieve the desired general holonomy which satisfies the compatibility condition in Theorem 3.5.

Conventional algorithms [3], [4], [33], [35] for flat cone metrics cannot produce metrics satisfying the holonomy constraint in Eqn.1. We observe that the flat cone metric on a polycube [37] satisfies the compatibility condition in Eqn.1 for 4-RoSy fields. The flat metric on a mesh with all faces being equilateral triangles is compatible with 6-RoSy fields.

The following algorithm computes the desired flat cone metric for genus zero surfaces based on the polycube map method introduced in [38].

1) First, the user specifies the singularities of the N-RoSy field for both positions and indices, such that the curvatures satisfy the holonomy condition in Eqn.1 and are positive. Furthermore, the user specifies the connectivity of a polyhedron P, whose vertices are the cone singularities, and faces are either quadrilaterals or triangles.
2) We use the discrete Ricci flow method [4] to compute a flat cone metric. If $\{s_i, s_j\}$ is an edge in P, we compute the shortest path connecting s_i, s_j under the flat metric. P is decomposed to segments by the line segments.
3) Each segment is deformed to a rectangle or a equilateral triangle by discrete Ricci flow. For example, if we set the boundary curvature at the corners to be $\frac{\pi}{2}$ and zero everywhere else for a segment, then the metric obtained from the Ricci flow makes the segment a rectangle.
4) We assembly the rectangles (equilateral triangles) to the polycube. By scaling the polycube along x-axis,y-axis and z-axis respectively, we make its holonomy compatible to the conditions in Theorem 3.5.

For more details for constructing polycubes (especially for high-genus models), we refer readers to [38].

Figure 1 illustrates several remeshing results based on the metric compensation. Frame (a) and (b) show a 3-RoSy field and a 4-RoSy field on the buddha model respectively. In frame (c), a flat cone metric deforms the mesh in the shape of an obelisk, which induces a mixed 4-RoSy and 3-RoSy field on the mesh. Frame (d) shows a mixed quadrilateral and triangle tessellation based on the flat cone metric illustrated in Frame (c). As illustrated, we construct a 12-Rosy field on the Buddha model with 9 singularities. The curvatures are 90 degrees for the bottom 4 singularities, 60 degrees for the middle 4 cones and 120 degrees for the apex. On the pyramid of the obelisk, we show the 3-RoSy field; on the rest part of the obelisk, we show the 4-RoSy field. Frame (e) shows a quad-remeshing result corresponding to the field in Frame (b). Note that some cone singularities around the shoulder are negative, which can be handled by our method consistently. The Celtic knot in Frame (f) is constructed based on the quad-remeshing in frame (e).

4.2 N-RoSy Field Editing

Suppose users add some geometric constraints to the N-Rosy field, our method can incorporate them easily. We decompose the constraints as orientation constraints and length constraints. Suppose the user specifies the directions of the vectors at special point set $\omega \subset M$. For each vertex q on M, assume that the angle between the current angle $\mathbf{w}(q)$ and the edited direction given the constraints is $\psi(q)$. Let $p \in \omega$ with user specified guiding vector, the angle between $\mathbf{w}(p)$ and the desired direction is $\bar{\psi}(p)$. For the N-RoSy field with $N > 1$, any direction from the multi-valued directions is valid. We normally choose the one closest to $\mathbf{w}(p)$ to reduce introduced rotations. Then we compute a harmonic function using the method described in [25] $\psi : M \to \mathbb{R}$ with the boundary condition on Ω. This leads to the well-known Laplacian equation with the Dirichlet boundary conditions. For each point $q \in M$, the following holds

$$\Delta\psi(q) = \sum_{<q,r> \in M} w_{qr} \left(\psi(r) - \psi(q)\right) = 0,$$

where Δ is the discrete Laplacian-Beltrami operator, and w_{qr} is the cotangent weights [39]. For each hard constraint at vertex p, we simply replace $\Delta\psi(p) = 0$ with the constraint $\psi(p) = \bar{\psi(p)}$. For a soft constraint at p that only need to satisfy in the least-squares sense, we add $\lambda\psi p = \lambda\bar{\psi}(p)$ to the

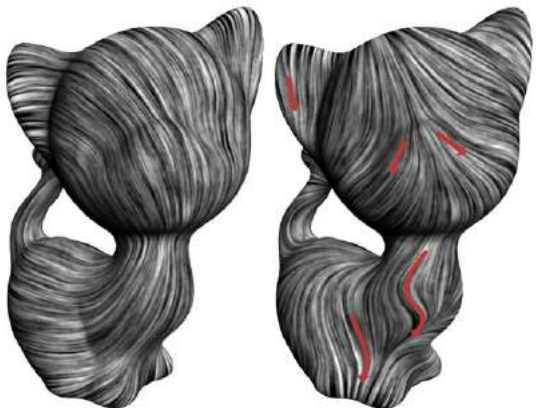

Fig. 11: *Vector field editing.*

linear system to form an over-determined system, where λ is the relative importance of given constraint. We may compute the least-squares solution to this linear system, which amounts to minimizing a combination functional of the Dirichlet energy and given constraints.

After solving the linear system, at each point $q \in M$, we rotate $\mathbf{w}(q)$ by an angle $\psi(q)$. The length constraint can be satisfied using the similar harmonic function method. It is clear that harmonic interpolation of directions won't generate any new singularities. Given the user-defined length constraints (by default, lengths are positive), the harmonic length interpolation will generate a field without any additional singularities, due to the maximum principle of harmonic function. Compared with the method in [15], we both lead to a least-squares problem which can be efficiently solved. While the fundamental difference is that our method smoothly alters an initially smooth N-RoSy field, thus it is guaranteed that no extra singularities will be introduced; on the contrary, extra singularities may emerge in their method.

Figure 11 demonstrates a vector field editing process on the kitten surface. The red arrows are specified directions, and the vector field is modified to follow these directions. The computation of N-RoSy field editing just takes a fraction of second on commodity PCs (cf. Table 1) and thus can be performed interactively.

4.3 Handling Open Meshes

Our method can easily handle meshes with open boundaries. If the N-RoSy field can be arbitrary at the boundary, we simply need to compute a flat cone metric of the mesh and the further processing is the same. To compute the flat cone metric with Ricci flow, the Gaussian curvature for each boundary vertex should be prescribed, just as the cone singularities. The Gaussian curvature at a boundary vertex v is determined by $K_v = \pi - \sum \tau_i$, where τ_i are top angles of 1-ring neighbors of v. For our purpose, the curvatures at boundaries and cone singularities may be chosen rather arbitrarily, as long as the total Gaussian curvature satisfies Gauss-Bonnet theorem. If the N-RoSy field is desired to be along the boundaries, we may use the concept of double covering to easily solve this [40]. We first make a duplication of the input mesh but with the orientation of all the faces inverted, and then glue the duplicated version together with the input open mesh to form a symmetric closed mesh. For the newly created mesh, it can be processed in the usual way, but keep in mind that each singularity appears twice on both submeshes simultaneously. We use the derived N-RoSy field on the original half of the mesh as the output. Due to the symmetry, we may verify that the N-RoSy field should be parallel to the boundaries. If, on the other hand, the N-RoSy field is desired to be orthogonal to the boundaries, we may rotate the field by 90 degrees using hodge star operator.

In this section, practical algorithms for N-RoSy field design and remeshing are discussed. To eliminate jumps around handles or singularities, either rotation compensation or metric compensation can be used. Neither of these methods will generate any additional singularities. Rotation compensation locally rotates the vector field according to a smooth harmonic function. It's clear that this process will not generate excessive singularities (vectors with vanishing length). For metric compensation, the constructed polycubes just contain the specified singularities. Therefore, our method is completely free of unwanted additional singularities. For constructing smooth N-RoSy fields, rotation compensation is generally enough. In this case, the only user inputs are the positions and indices of the singularities, all the other steps are completely automatic. Furthermore, the inputs of singularities can be obtained from other fields directly, such as the principal direction fields etc. Therefore, the system can be fully automatic. If user interaction is desired, the system allows users to give more inputs to edit the field. Metric compensation approach requires slightly more information, but it not only compensates for the rotational component of holonomy, but also the generalized holonomy that satisfies the compatibility condition in Theorem 3.5 and admits regular remeshing.

5 Experimental Results

We implemented our algorithm in C++ on an Intel Core2Duo 2GHz Laptop with 2GB memory. We report the timings for the major steps in Table 1, which include the computations for the flat metric, rotational compensation, and user editing. The flat metric computation accounts for most of the time. Although the Ricci flow method is non-linear, using the Newton solver described in [4], the performance can be greatly improved. For moderately sized models, sufficiently fast feedback can be given, allowing interactive changing of singularities. The rotation compensation and feedback to editing are linear and can be performed at an interactive rate. Also, if no user editing is involved, the whole pipeline is fully automatic, after singularities are specified, or derived from some field (e.g. principal tensor fields).

Remeshing In the holonomy compensation step of stage one (section 4.1.3), we use the metric compensation method to

adjust the metric to satisfy the tessellation compatibility condition in Theorem 3.5. Then we develop the mesh to the plane, and tessellate the development. This induces a desired tessellation.

Figure 1 demonstrates the results of N-RoSy field on the buddha model. Frame (a) and (b) show a 3-RoSy field and a 4-RoSy field on the buddha model respectively. In frame (c), a flat cone metric deforms the mesh in the shape of an obelisk, which induces a mixed 4-RoSy and 3-RoSy field on the mesh. (d) shows a mixed quadrilateral and triangle tessellation based on the flat cone metric. The Celtic knot in the last frame is constructed based on the quad-remeshing in frame (e).

Celtic Knot on Surface Celtic knot refers to a variety of endless knots, which in most cases contain delicate symmetries and entangled structures. Figure 12 shows a simple Celtic knot. To the best of our knowledge, Kaplan and Cohen [26] were the first to present a technique for computer generated Celtic design. Most of their results focused on planar Celtic knot design, whereas our work emphasizes Celtic knots woven over surfaces with highly global symmetry. Celtic knot produced by our method is based on regular remeshing. They are geometric textures represented as surfaces with tens of thousands of face.

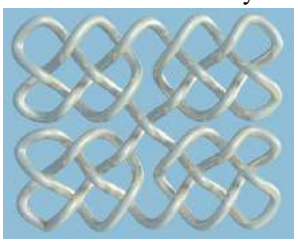

Fig. 12: A planar Celtic knot.

The local symmetry and the quality of remeshing of the surfaces play crucial roles for the knotwork on surfaces. Based on our remeshed results, those uniform quads and triangles provide a perfect canvas for Celtic knot design. Similar to the method in [26], we set control points directly on surfaces, connecting them using polynomials based on the knot designing rules. Compared with traditional geometric texture synthesis approaches, we do not need shell mapping from planar domains to surfaces. Figures 1,13,16 show our Celtic knots synthesis results on several surfaces. The knotwork has complicated structures and rich symmetries. In the last example, celtic knots are woven with colored threads only over Bimba's body due to the aesthetic concern, mimicking the dressed sweater.

Pen-and-ink Sketching of Surfaces Pen-and-ink sketching of surfaces is a non-photorealistic style of shape visualization. In this work, we follow Hertzmann and Zorin [16] by treating

TABLE 1: *Running times for different steps of our algorithm. (F-No. of faces, g-genus, s- No. of singularities)*

Model	F	g	s	Metric(s)	Comp.(s)	Edit(s)
kitten	19350	1	0	1.198	0.078	0.410
amphora	20078	2	1	2.164	0.266	0.452
venus	20308	0	5	1.843	0.087	0.453
bimba	22412	0	6	1.426	0.098	0.522
3holes	3514	3	4	0.320	0.157	—
Pensatore(3-RS)	21304	0	6	1.436	0.079	—
Pensatore(4-RS)	21304	0	8	1.431	0.083	—
Buddha(3-RS)	20828	0	6	1.480	0.078	—

Fig. 13: *Two woven Celtic knot designs on the Moai surface, which have different global symmetries.*

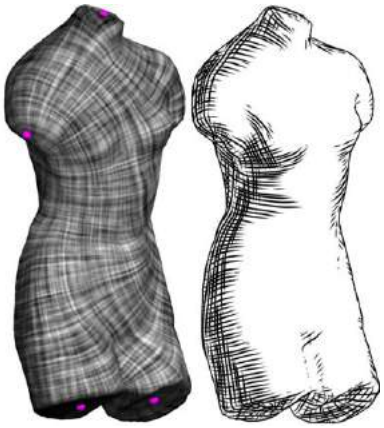

Fig. 14: *Pen-and-ink sketching of venus model.*

hatch directions as a 4-RoSy field.

Our method neither requires the user to input an initial field, nor generates excess singularities except those specified by the user. It enables the user to fully control the number, positions and the indices of singularities, and edit the field interactively. These merits make our system rather desirable for NPR applications.

For example, we perform the pen-and-ink sketching on the Venus model in Figure 14 and Bimba model in Figure 15. The left columns show the 4-RoSy fields with user specified singularities, 6 for Bimba, 5 for Venus. Comparing with the algorithm in [1], our method reduces the number of singularities by one order of magnitude, and locates them at the natural positions. This greatly reduces the visual artifacts and simplifies the designing process. The editing process improves the hatching quality on the Bimba model shown in 15.

More experimental results are reported in our supplementary video.

6 Conclusions

This work introduces rigorous and practical algorithms for automatic N-RoSy field design on arbitrary surfaces with prescribed topologies. The user has full control of the number, positions and indices of the singularities (as long as necessary

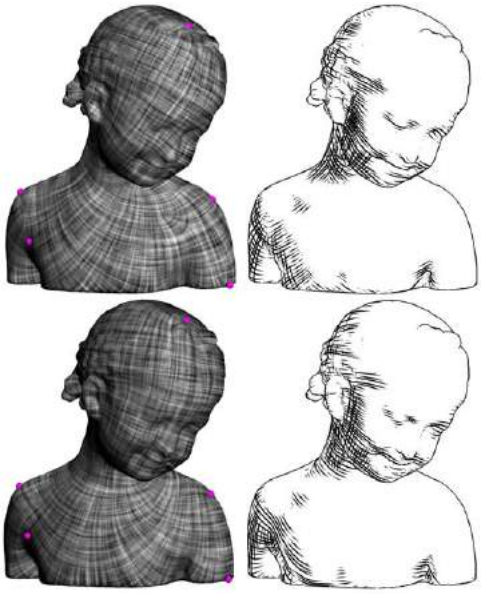

Fig. 15: *Pen-and-ink sketching of bimba before (top row) and after editing (bottom row). The hatch directions follow the natural directions better (e.g. neck,arm).*

global constraints are satisfied), as well as the turning numbers of the loops.

We have also proved the compatibility condition between the metric and N-RoSy fields (and regular tessellation). Based on the theoretical findings, we turn the problem of N-RoSy field design to a metric design problem with constrained holonomy. By changing the metric of the surface, we enforce the global symmetry of the surface to be compatible with the local symmetry of the N-RoSy field. By using the flat cone metric, we greatly reduce the complexity of the design process. We also generalize the method for tessellation and mixed N-RoSy field design.

We applied our algorithm for NPR rendering, remeshing, and geometric texture synthesis. We develop a global approach to design Celtic knot on surfaces.

Some limitations still exist in our approach. The major limitation is our method is based on Ricci flow to compute flat cone metrics with specified singularities. This method is non-linear, and compared with linear methods (e.g. based on 1-forms), this method is relatively slower. Using Newton solver speeds up the computation, but is still slower than linear methods. For applications that requires larger model or faster feedback, we may explore parallel multigrid solvers to further improve the performance.

Metric design is a very general approach, and we believe that it has potential of being applied for many other graphics tasks, such as parameterizations, mesh editing, and efficient rendering, etc. Our work demonstrates the effectiveness of using flat cone metrics to produce high quality N-RoSy fields. We also conjecture N-RoSy fields can be utilized to produce a special flat cone metric. In the future, we will explore further in these directions.

REFERENCES

[1] J. Palacios and E. Zhang, "Rotational symmetry field design on surfaces," *ACM Trans. Graph.*, vol. 26, no. 3, p. 55, 2007.

[2] N. Ray, B. Vallet, W.-C. Li, and B. Levy, "N-symmetry direction field design," vol. 27, no. 2, pp. 10:1–10:13, 2008.

[3] L. Kharevych, B. Springborn, and P. Schröder, "Discrete conformal mappings via circle patterns," *ACM Trans. Graph.*, vol. 25, no. 2, pp. 412–438, 2006.

[4] M. Jin, J. Kim, F. Luo, and X. Gu, "Discrete surface ricci flow: Theories and applications," in *Mathematics of Surfaces XII*, ser. Lecture Notes in Computer Science, vol. 4647. Springer, 2007, pp. 209–232.

[5] E. Praun, A. Finkelstein, and H. Hoppe, "Lapped textures," *Proc. ACM/SIGGRAPH Conf.*, pp. 465–470, Aug. 2000.

[6] G. Turk, "Texture synthesis on surfaces," in *Proc. ACM/SIGGRAPH Conf.*, 2001, pp. 347–354.

[7] L. Y. Wei and M. Levoy, "Texture synthesis over arbitrary manifold surfaces," *Proc. ACM/SIGGRAPH Conf.*, pp. 355–360, 2001.

[8] J. Stam, "Flows on surfaces of arbitrary topology," *Proc. ACM/SIGGRAPH Conf.*, vol. 22, no. 3, pp. 724–731, Jul. 2003.

[9] J. J. van Wijk, "Image based flow visualization," *Proc. ACM/SIGGRAPH Conf.*, vol. 21, no. 3, pp. 745–754, Jul. 2002.

[10] J. J. van Wijk, "Image based flow visualization for curved surfaces," *Proc. IEEE Vis.*, pp. 123–130, Oct 2003.

[11] H. Theisel, "Designing 2d vector fields of arbitrary topology," in *Proc. Eurographics*, vol. 21, 2002, pp. 595–604.

[12] E. Zhang, K. Mischaikow, and G. Turk, "Vector field design on surfaces," *ACM Trans. Graph.*, vol. 25, no. 4, pp. 1294–1326, 2006.

[13] G. Chen, K. Mischaikow, R. S. Laramee, P. Pilarczyk, and E. Zhang, "Vector field editing and periodic orbit extraction using morse decomposition," *IEEE Trans. Vis. Comp. Graph.*, vol. 13, no. 4, pp. 769–785, 2007.

[14] E. Zhang, J. Hays, and G. Turk, "Interactive tensor field design and visualization on surfaces," *IEEE Trans. Vis. Comp. Graph.*, vol. 13, no. 1, pp. 94–107, 2007.

[15] M. Fisher, P. Schröder, M. Desbrun, and H. Hoppe, "Design of tangent vector fields," *ACM Trans. Graph.*, vol. 26, no. 3, p. 56, 2007.

[16] A. Hertzmann and D. Zorin, "Illustrating smooth surfaces," *Proc. ACM/SIGGRAPH Conf.*, pp. 517–526, Aug. 2000.

[17] N. Ray, W. C. Li, B. Lévy, A. Sheffer, and P. Alliez, "Periodic global parameterization," *ACM Trans. Graph.*, vol. 25, no. 4, pp. 1460–1485, 2006.

[18] Y. Tong, P. Alliez, D. Cohen-Steiner, and M. Desbrun, "Designing quadrangulations with discrete harmonic forms," in *Proc. Symp. Geom. Proc.*, 2006, pp. 201–210.

[19] F. Kälberer, M. Nieser, and K. Polthier, "Quadcover - surface parameterization using branched coverings," *Comp. Graph. Forum*, vol. 26, no. 10, pp. 375–384, Sep 2007.

[20] A. Girshick, V. Interrante, S. Haker, and T. Lemoine, "Line direction matters: an argument for the use of principal directions in 3D line drawings," *Proc. NPAR*, pp. 43–52, 2000.

[21] M. Meyer, M. Desbrun, P. Schröder, and A. H. Barr, "Discrete differential-geometry operators for triangulated 2-manifolds," *VisMath*, 2002.

[22] D. Cohen-Steiner and J. Morvan, "Restricted delaunay triangulations and normal cycle," in *Proc. ACM Symp. Comp. Geom.*, 2003, pp. 312–321.

[23] S. Rusinkiewicz, "Estimating curvatures and their derivatives on triangle meshes," in *Proc. 3DPVT*, 2004, pp. 486–493.

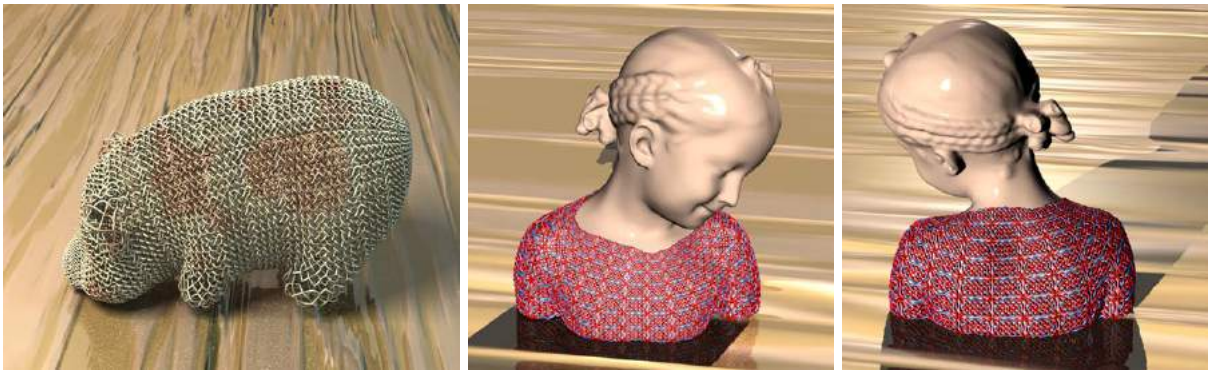

Fig. 16: *Celtic knots designed surfaces.*

[24] S. Zelinka and M. Garland, "Jump map-based interactive texture synthesis," *ACM Trans. Graph.*, vol. 23, no. 4, pp. 930–962, 2004.

[25] X. Ni, M. Garland, and J. C. Hart, "Fair morse functions for extracting the topological structure of a surface mesh," *ACM Trans. Graph.*, vol. 23, no. 3, pp. 613–622, 2004.

[26] M. Kaplan and E. Cohen, "Computer generated celtic design," in *Proceedings of the 14th Eurographics Workshop on Rendering Techniques*, 2003, pp. 2–19.

[27] K. Zhou, X. Huang, X. Wang, Y. Tong, M. Desbrun, B. Guo, and H.-Y. Shum, "Mesh quilting for geometric texture synthesis," *ACM Trans. Graph.*, vol. 25, no. 3, pp. 690–697, 2006.

[28] P. Alliez, D. Cohen-Steiner, O. Devillers, B. Lévy, and M. Desbrun, "Anisotropic polygonal remeshing," *ACM Trans. Graph.*, vol. 22, no. 3, pp. 485–493, Jul. 2003.

[29] M. Marinov and L. Kobbelt, "Direct anisotropic quad-dominant remeshing," *Proc. Pacific Graph.*, pp. 207–216, 2004.

[30] S. Dong, S. Kircher, and M. Garland, "Harmonic functions for quadrilateral remeshing of arbitrary manifolds," *CAGD*, no. 5, pp. 392–423, 2005.

[31] S. Dong, P.-T. Bremer, M. Garland, V. Pascucci, and J. C. Hart, "Spectral surface quadrangulation," *ACM Trans. Graph.*, vol. 25, no. 3, pp. 1057–1066, 2006.

[32] R. S. Hamilton, "Three-manifolds with positive ricci curvature," *J. Diff. Geom.*, vol. 17, pp. 255–306, 1982.

[33] M. Ben-Chen, C. Gotsman, and G. Bunin, "Conformal flattening by curvature prescription and metric scaling," *Comp. Graph. Forum*, vol. 27, no. 2, pp. 449–458, 2008.

[34] F. Luo, "Combinatorial Yamabe flow on surfaces," *Communications Contemporary Mathematics*, vol. 6, pp. 765–780, 2004.

[35] B. Springborn, P. Schröder, and U. Pinkall, "Conformal equivalence of triangle meshes," *ACM Trans. Graphics*, vol. 27, no. 3, p. article no. 77, 2008.

[36] K. Polthier and M. Schmies, "Straightest geodesics on polyhedral surfaces," in *Proc. Mathematical Visualization*, 1998, pp. 391–398.

[37] M. Tarini, K. Hormann, P. Cignoni, and C. Montani, "Polycube-maps," *ACM Trans. Graph.*, vol. 23, no. 3, pp. 853–860, 2004.

[38] H. Wang, Y. He, X. Li, X. Gu, and H. Qin, "Polycube splines," in *Proc. ACM Symp. Solid and Physical Modeling*, 2007, pp. 241–251.

[39] U. Pinkall and K. Polthier, "Computing discrete minimal surfaces and their conjugates," *Experimental Mathematics*, vol. 2, pp. 15–36, 1993.

[40] X. D. Gu and S.-T. Yau, "Global conformal surface parameterization," in *Proc. Symp. Geometry Processing*, 2003, pp. 127–137.

ACKNOWLEDGEMENTS

The models in this paper are courtesy of AIM@SHAPE Repository. This work was supported by the National Basic Research Project of China (Project Number 2006CB303102), the Natural Science Foundation of China (Project Number 60673004, 60628202). The project was also partially supported by NSF CCF-0841514, NSF CCF-0830550. Ying He was supported by the Singapore National Research Foundation Interactive Digital Media R&D Program, under research grant NRF2008IDM-IDM004-006.

APPENDIX

Theorem 3.1 *Suppose* $\mathbf{v}$ *is a smooth N-RoSy field on a surface* M *with an initial metric* $\mathbf{g}(0)$. $\mathbf{g}(t)$ *is a one parameter family of Riemannian metric tensors. Then for any closed loop* γ *on* M*, the relative rotation* $T_{\mathbf{v}}(\gamma)$ *on* $(M, \mathbf{g}(t))$ *is a constant for any* t*.*

Proof The Levi-Civita connections are continuously determined by $\mathbf{g}(t)$, therefore the parallel transport is continuously determined by $\mathbf{g}(t)$. The absolute rotation of $\mathbf{v}$ along γ, $R_{\mathbf{v}}(\gamma)$ is a continuous function of t, and so is the holonomic rotation of γ, $h(\gamma)$. We have that the relative rotation $T_{\mathbf{v}}(\gamma)$ is a continuous function. Because $\mathbf{v}$ is smooth on $(M, \mathbf{g}(0))$, therefore $\frac{N}{2\pi} T_{\mathbf{v}}(\gamma)|_{t=0}$ is an integer. Because it is also continuous, therefore, it must be a constant for all t. Since γ is chosen arbitrarily, the homotopy type of $\mathbf{v}$, the indexes of the singularities are preserved during the continuous metric deformation $\mathbf{g}(t)$. Q.E.D.

Theorem 3.2 *Suppose* M *is a surface with a flat cone metric. A parallel N-RoSy field exists on the surface, if and only if all the holonomic rotation angles of the metric are integer times of* $\frac{2\pi}{N}$*.*

Proof If the holonomic rotations of the flat cone metric are $\frac{2k\pi}{N}$, then parallel transporting an N-RoSy at the base point results in a field $\mathbf{v}$, $R_{\mathbf{v}}(\gamma) = 0$ for any loop γ. Consequently the compatibility is satisfied and the field is smooth. Reversely, if there exists a smooth parallel N-RoSy field $\mathbf{v}$, then $R_{\mathbf{v}}(\gamma)$ is zero for any loop γ. Therefore, $h(\gamma)$ must be integer times of $\frac{2\pi}{N}$. Q.E.D.

Corollary 3.3 *Suppose* M *is a genus zero closed surface with a finite number of cone singularities.* M *has a parallel N-RoSy field, if and only if the curvature for each cone singularity is* $\frac{2k\pi}{N}$*.*

Proof Let γ be a loop, which is the boundary of a region Ω on the surface. Suppose there are m cone singularities $\{s_1, s_2, \cdots, s_m\}$ inside Ω. According to Gauss-Bonnet theorem, the holonomic rotation angle of γ equals to the total curvature of Ω, $h(\gamma) = \sum_{i=1}^{m} k_i$, where k_i is the curvature of s_i. Let γ_i be a loop surrounding s_i without enclosing any other singularities, then $\{\gamma_i, i = 1, 2, \cdots, m-1\}$ is a set of generators of $\pi(M)$. M has a smooth parallel N-RoSy field, if and only if all $h(\gamma_i)'s$ are $\frac{2k\pi}{N}$. Q.E.D.

Theorem 3.4 *Suppose M is a surface with flat cone metric, then there exists a smooth N-RoSy field.*

Proof There exists a unique harmonic 1-form ω, such that $\int_\gamma \omega = h(\gamma)$, for any loop γ on $\bar{M}$. We parallel transport an N-RoSy from the base point, and rotate it during the transportation by an angle $\int_\gamma \omega$, where γ is any path from the base to the current point. The resulting field is smooth. Q.E.D.

Theorem 3.5 *Suppose M is with a flat cone metric, the holonomy group of $\bar{M}$ is $H(\bar{M})$, if $H(\bar{M})$ is a subgroup of G_T, then T can be defined on M.*

Proof Let $\tilde{M}$ be the universal covering space of $\bar{M}$. We equip $\tilde{M}$ with the flat cone metric and immerse $\tilde{M}$ onto the plane $\mathbb{R}^2$. Then the deck transformation group is a subgroup of the holonomy group $H(\bar{M})$. If T is a tessellation on $\mathbb{R}^2$, it is invariant under the action of G. $H(\bar{M})$ is a subgroup of G, so is the deck transformation group. Therefore, T is invariant under all the deck transformations of $\tilde{M}$, and so T can be defined on $\bar{M}$. Q.E.D.

For a mesh with a flat cone metric, homotopic loops have the same holonomy. It can be further proved that homologic loops have the same holonomy. But only homotopy loops have the same generalized holonomy. For the sake of simplicity, we don't introduce the concept of homology.

Yu-Kun Lai received his bachelor's degree and PhD degree in computer science from Tsinghua University in 2003 and 2008, respectively. He is currently a lecturer of visual computing in the School of Computer Science, Cardiff University, Wales, UK. His research interests include computer graphics, geometry processing, computer-aided geometric design and computer vision.

Miao Jin received her PhD in computer science from Stony Brook University in 2008. She is an assistant professor of the Center for Advanced Computer Studies (CACS), University of Louisiana at Lafayette. Her research interests include computational hyperbolic geometry, computational conformal geometry, and their applications in computer graphics, geometric modeling, and computer vision. Her major works include discrete Ricci flow, surface geometric structures, computational Teichmüller space, and global surface parametrization. For more information, see http://www.cacs.louisiana.edu/ mjin.

Xuexiang Xie received his BS degree in computer science in 1996 from Zhejiang University of China, and his PhD degree in computer engineering in 2009 from Nanyang Technological University of Singapore. His research interests include computer graphics, scientific visualization and computer vision. He is currently working on video-based modeling with applications in 3DTV.

Ying He received the Ph.D. degree in computer science from State University of New York (SUNY), Stony Brook, in 2006 and the M.S. and B.S. degrees in electrical engineering from Tsinghua University, China, in 2000 and 1997, respectively. He is currently an Assistant Professor at School of Computer Engineering, Nanyang Technological University, Singapore. His research interests include computer graphics, computer-aided design and scientific visualization. For details, please visit http://www.ntu.edu.sg/home/yhe.

Jonathan Palacios is currently a Ph.D. student in the Department of Electrical Engineering and Computer Science at Oregon State University, studying under Dr. Eugene Zhang. His primary research areas are computer graphics, geometric modeling, symmetry, and higher-order tensor field visualization and analysis. He is an NSF IGERT fellow, and a a member of the ACM.

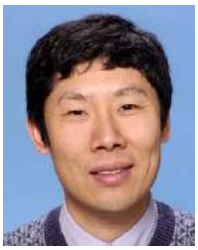

Eugene Zhang received the PhD degree in computer science in 2004 from Georgia Institute of Technology. He is currently an assistant professor at Oregon State University, where he is a member of the School of Electrical Engineering and Computer Science. His research interests include computer graphics, scientific visualization, and geometric modeling. He received an National Science Foundation (NSF) CAREER award in 2006. He is a member of the IEEE and ACM.

Shi-Min Hu received the PhD degree from Zhejiang University, in 1996. He is currently a chair professor of computer science in the Department of Computer Science and Technology, Tsinghua University, Beijing. His research interests include digital geometry processing, video processing, rendering, computer animation, and computer-aided geometric design. He is on the editorial boards of Computer Aided Design. He is a member of the IEEE.

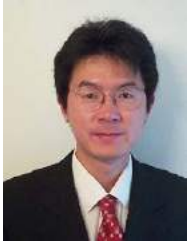

Xianfeng Gu received the PhD in computer science from Harvard University in 2003. He is an assistant professor of computer science at State University of New York at Stony Brook. He won the US National Science Foundation CAREER award in 2004. His research interests include computational conformal geometry, and their applications in computer graphics, computer vision, and medical imaging. His major works include geometry images, global conformal surface parameterization, manifold splines, discrete Ricci flow and discrete Yamabe flow. For more information, see http://www.cs.sunysb.edu/gu.